

DNS of Syngas Autoignition In Stratified Medium

Rahul Patil¹, Sheshadri Sreedhara¹

¹IC Engines and Combustion Laboratory,
Department of Mechanical Engineering,
Indian Institute of Technology Bombay, Mumbai 400076, India
aarpatil@iitb.ac.in

Abstract – This paper presents an analysis of syngas combustion using 2D Direct Numerical Simulation (DNS) near Homogeneous Charge Compression Ignition (HCCI) conditions. The study examines combustion phasing achieved through varying levels of stratification which were generated within the domain to replicate different mixture distributions resulting from incomplete mixing of fuel and oxidizer streams. Simulations were categorized into two types: thermal stratification, which mimics the effect of wall cooling, and compositional stratification, which simulates the effects of evaporative cooling of cold fuel. The impact of these stratifications on the combustion dynamics was analyzed. The simulations were conducted under HCCI-relevant initial conditions (1070 K and 41 bar) using syngas as the fuel having an equimolar mixture of H₂ and CO. A detailed chemical mechanism involving 21 species and 93 reactions was employed to simulate syngas autoignition. The study found that combustion phasing due to stratification resulted in two distinct combustion modes viz. volumetric ignition and deflagration. Results indicated that H₂, being more reactive, was consumed earlier than CO. Thermal stratification led to smoother combustion with increased mixing or temperature fluctuations, while compositional stratification resulted in combustion behavior closer to homogeneous autoignition.

Keywords: DNS, HCCI, Syngas, autoignition, deflagration

1. Introduction

Homogeneous charge compression ignition (HCCI) is a promising new technology that can achieve efficient and ultra-low emissions. However, the development of the HCCI engine has not been realized due to a shortcoming of knowledge of fundamental issues such as control of the combustion phasing. The combustion phasing for the HCCI engine is mainly controlled by compositional or thermal stratification. The mixture stratification offers efficiency and can burn the mixture at overall ultra-lean mixture compositions. This feature makes it desirable for efficient and cleaner combustion devices. Exhaust gas recirculation [1] or direct injection [2] inside the combustion chamber can achieve compositional stratification. The cooling of the combustion chamber walls corresponds to the thermal stratification inside the combustion chamber. The turbulence created due to charge intake breaks down larger stratification scales into smaller ones. Most DNS studies on HCCI mainly focus on understanding ignition and combustion behavior at these small scales [1]–[3]. The HCCI or low temperature combustion (LTC) primarily occurs in two ignition modes, i.e., flame propagation (deflagration) or volumetric ignition (spontaneous ignition).

The working strategy for engines operating on these technologies must account for both combustion modes. The ignition spots originate from locations with lower scalar dissipation rates and the most reactive mixture [4]. The deflagration waves originate from ignition spots and consume the charge within the domain. The experimental studies performed to analyze deflagration waves do not give conclusive results related to the propagation speed of deflagration waves. The ignition front originating from the ignition spot can take various forms of ignition, such as explosion, supersonic deflagration, detonation, subsonic deflagration, and laminar deflagration. Gu et al. [5] showed that the ignition front can be classified based on the initial slope of thermal stratification.

During injection of fuel to combustion chamber, the composition of the mixture formed inside the combustion chamber is mostly non-correlated to temperature. The temperature inside the combustion chamber is generally higher than the injected fuel temperature. With time advancement, the equivalence ratio field starts to negatively correlate with temperature due to evaporative cooling of the mixture.

In this study, the effect of stratification on combustion dynamics is presented by analyzing two types of mixture distribution fields. Those fields are 1) thermal stratification (due to wall cooling) and 2) negatively correlated compositional stratification (due to evaporative cooling).

The present study is performed with 2D DNS configuration. This study does not focus on the cascading of energy spectra, so the 2D approximation of the flow field can be used. Sreedhara and Lakshmisha [4] have compared 2D and 3D DNS, and they observed that due to higher dissipation in 3D DNS (more accurate), lower ignition delay was observed compared to 2D DNS. Ameen and Abraham [6] also added that 2D DNS can be used for qualitative assessment of combustion. The capability of 2D DNS to capture the corrugation of wrinkling flame structure gives physical relevance to the solution obtained from the simulations. In previous studies, such as Pal et al. [7], the 2D DNS had been used to calculate the combustion regime for the autoignition of syngas. The study presented by Karimkashi et al. [8] captured the effect of convective mixing of dual fuel composition using 2D DNS. These studies indicate that 2D DNS is also sufficient to investigate the combustion.

The present study presents an analysis with 2D DNS to identify the effects of stratification on flame dynamics. A Damkohler number-based analysis will be performed in the future to identify the propagation speeds of deflagration waves under various stratification conditions. The effect of variation in mixture reactivity and mass diffusivity of fuel components on flame dynamics are also presented. In the present study, the global mean equivalence ratio ($\langle\phi\rangle$) equal 0.1 was used. overall lean mixture with equivalence ratio fluctuations (ϕ') 0.05 and 0.1 were simulated. The initial conditions are kept close to the HCCI relevant conditions: mean temperature =1070 K and pressure =41 bar.

2. Numerical setup and problem definition

2D Direct Numerical Simulations (DNS) with decaying turbulence were simulated in this study, using a square domain of $0.41 \times 0.41 \text{ cm}^2$ size. The simulations were performed with open-source PENCIL code [9]. A 6th-order compact scheme was used for spatial differentiation, and the time marching was performed using the LSODE solver. The domain was divided into 960×960 grids, having a grid resolution of $4.3 \text{ }\mu\text{m}$. The resolution was sufficient to resolve thin deflagration waves [10], [11]. The periodic boundary conditions were imposed along the x and y directions of the domain. The initial conditions were kept close to autoignition conditions i.e., pressure equal to 41 bar and temperature equal to 1070 K. The velocity fluctuations were imposed on zero mean velocity. The initial velocity and species fields were imposed with the help of the Passot-Pouquet spectrum given by [12].

$$E(k) = \frac{32}{3} u' \sqrt{\frac{2}{\pi}} \left(\frac{k^4}{k_0^5} \right) \exp \left(-2 \left(\frac{k}{k_0} \right)^2 \right) \quad (1)$$

where u' is the root mean square (RMS) of velocity fluctuation, k is the wave number, and k_0 is the most energetic wavenumber. The Initial auto-correlation between the most energetic scale and the initial integral scale L_i is given by

$$k_0 = \frac{1}{L_i \sqrt{2\pi}} \quad (2)$$

The effect of the initial distribution of equivalence ratio and temperature field on combustion is investigated in this study. The stratification used in this study can be classified into two categories of 6 cases of DNS. The initial set of DNS cases corresponds to thermal stratification, where a temperature field was imposed on the domain. The other set corresponds to compositional stratification that negatively correlates with thermal stratification. The details of the cases are summarized in Table 1. The columns given in the table are corresponding to l_ϕ (integral scale for equivalence ratio distribution), l_T (integral scale for temperature distribution), ϕ'/ϕ is the ratio of root mean square value of equivalence ratio to mean equivalence ratio, T' is the root mean square value of temperature fluctuations, and l_d is the length of the domain. The cases with compositional stratification with negative temperature correlation are represented by -NC (negatively correlated) in the table. The field imposed here was initiated with the same Passot-Pouquet spectrum given by Eq. 1. The wave number associated with the most energetic scale had been varied based on the integral scale of the distribution of

temperature and equivalence ratio. u' from Eq. 1 was replaced with T' and ϕ' based on temperature and compositional stratification.

Table 1: Parameters used for initial distribution equivalence ratio.

Case	Compositional stratification		Thermal stratification	
	l_ϕ/l_d	ϕ'/ϕ	l_T/l_d	$T'(K)$
A	--	--	0.1	15
B	--	--	0.2	15
C	--	--	0.1	30
A-NC	0.1	0.5	0.1	15
B-NC	0.2	0.5	0.2	15
C-NC	0.1	1.0	0.1	30

The initial distributions corresponding to thermal stratified fields (a-c) and compositionally stratified fields (d-f) are shown in Fig. 1. The compositionally stratified cases have temperature fields similar to the thermally stratified cases, but ϕ is negatively correlated to the temperature field. However thermally stratified cases (a-c) have uniform equivalence ratio distribution.

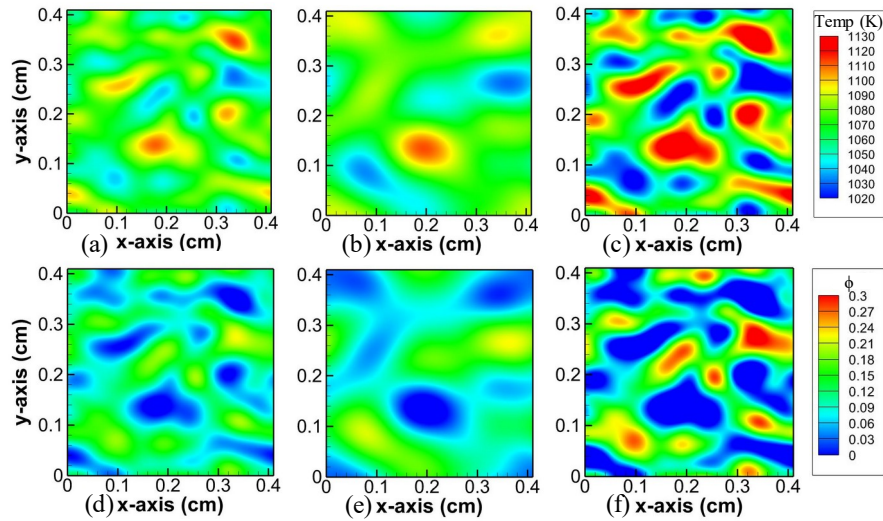


Fig. 1 Initial distribution of equivalence ratios and temperature fields for (a) case A, (b) case B, (c) case C, (d) case A-nc, (e) case B-nc, (f) case C-nc

A comprehensive study of various reaction mechanisms of syngas performed by Olm et al.[13] indicated that the mechanism by Li et al. [14] performed realistically well in predicting ignition delays for various compositions, temperatures, and pressure conditions for syngas. An equimolar mixture of H_2 and CO is used as the fuel to simulate the combustion of syngas. The chemical mechanism for syngas involving 21 species and 93 reactions was used in the present study [14]. The velocity field with u' equal to 50 cm/s is imposed on the domain.

Mathematical formulation

The flame originates from a spontaneous autoignition site and propagates via a deflagration wave. Deflagration wave dynamics can be studied if the deflagration waves are separated from autoignition sites. Since the autoignition sites co-existed with deflagration waves, the analysis without separation of combustion mode may show an overlap between the effects of autoignition and deflagration. Various studies have been presented to distinguish the mode of combustion such as

Sankaran number [15], Damkohler number (Da) [11], etc. The steady propagating deflagration wave maintains a balance between reaction and diffusion terms of the species transport equation. The Da based on reaction and diffusion term of species transport can be used to distinguish spontaneous autoignition and deflagration modes of combustion. In this analysis, HO_2 is used as a marker-species for differentiating between combustion modes. The definition of Da based on HO_2 is given as

$$Da = \frac{|\max(\dot{\omega}_{HO_2})|}{|\max(-\nabla \cdot (\rho Y_{HO_2} D))|} \quad (3)$$

where $\dot{\omega}_{HO_2}$ and Y_{HO_2} are the reaction rate and mass fraction of HO_2 , respectively, ρ represents density, and D is the diffusivity. The results showed that the reaction component was more prominent for the autoignition sites compared to the diffusion component. Based on this observation, the first order Da , which was close to 3.8, was used to separate the modes of combustion [2].

3. Results and Discussion

3.1. 0D simulation

The ignition characteristics for syngas combustion at $\phi=0.1$, $T=1070$ K, and $P=41$ bar at constant volume was formulated by 0D simulations performed using Chemkin [16]. The temporal evolution of species and HRR can be observed in Fig. 2. The figure shows that the HRR shows a steep incline in the region where the consumption rate of H_2 species is higher. The HRR is observed to be shallower at instant when a higher consumption rate of CO was observed. The fuel species H_2 is observed to be consumed earlier than CO . The species build-up observed for H_2O_2 and HO_2 species is similar to H_2 autoignition. Comparatively, H_2O_2 species are observed to accumulate faster compared to HO_2 species. The higher consumption of H_2O_2 species is observed as the mixture becomes closer to peak HRR. With the increase in temperature, H_2O_2 species were consumed by the exothermic reaction, forming OH species. The reactions release significant heat which aids in the oxidation of OH species, resulting in rapid HRR. On the other hand, the accumulated HO_2 species show a steady presence even when depletion of H_2 is observed. The presence of HO_2 throughout the evolution of autoignition makes it suitable to use Da based analysis to separate the combustion modes.

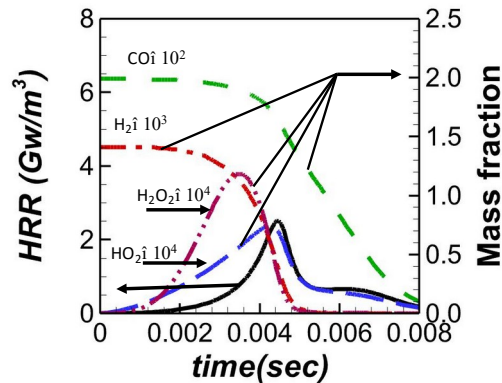


Fig. 2 Temporal evolution of heat release rate (HRR), species mass fractions.

3.2. 2D simulation

The temporal evolution of mean HRR and fuel species consumption across the domain for various cases can be observed in Fig. 3. The HRR shown in this figure is averaged over the domain. The HRR for 2D cases follows a trend similar to the HRR obtained in 0D simulations. Furthermore, the fuel species consumption rates also show a trend similar to 0D simulations. Fig. 3 also indicates the temporal evolution of fuel species H_2 and CO consumption rate. The fuel species H_2 has consumed earlier compared to CO due to its higher reactivity. The peak consumption rate of H_2 is also higher than CO . The peak CO consumption rate is also observed close to the peak H_2 consumption rate, maintaining a plateau-like nature after that and tapering to the minimum value. Due to the lower reactivity of fuel species CO , the heat released from H_2 combustion might have accelerated the CO oxidation reaction.

For thermally stratified cases (case A-C), with an increase in l_T/l_d or T' , resulted in earlier peak HRR compared to the 0D case. The increase in l_T/l_d or T' , also resulted in broader HRR profiles with reduced peak HRR values. The figure shows a reduced peak and broader distribution of the HRR profile, emphasizing that the cases with thermal stratification give smoother combustion compared to homogenous autoignition. In contrast, NC cases result in a sharper rise and higher magnitude of peak HRR values. The enhanced reactivity of the mixture due to the presence of a hot spot might be a reason behind the earlier evolution of the HRR profile in thermally stratified cases. For the -NC case, the enhancement of reactivity due to the presence of richer (compared to mean $\phi=0.1$) is nullified due to the reduction in temperature due to the negative correlation between temperature and ϕ . With an increase in l_ϕ/l_d or ϕ'/ϕ , -NC cases show a reversed trend for HRR distribution compared to thermally stratified cases. An increase in l_ϕ/l_d or ϕ'/ϕ resulted in a delayed and sharper HRR profile.

The variation in the consumption rate of fuel species with variation in stratification can also be seen in Fig. 3. The consumption rates of cases with thermal stratification are observed to have wider fuel consumption profiles with lower peaks. In contrast, the -NC cases have narrower distributions with larger peaks. The cases with thermal stratification enhance reactivity due to increase in localized temperature. The enhanced reactivity results in earlier ignition for case C compared to 0D case and case A. For case C, the earlier consumption of H_2 also in availed energy for CO oxidation reaction resulted in earlier CO consumption. With variation in thermal stratification, large variations are observed in peak H_2 consumption compared to peak CO consumption. On the other hand, for -NC cases with variation in compositional stratification, the variation in peak CO consumption rate is more pronounced compared to H_2 consumption rate. A sharper rise in H_2 consumption results in more energy available for CO oxidation and a faster depletion of CO is observed in the C-NC case.

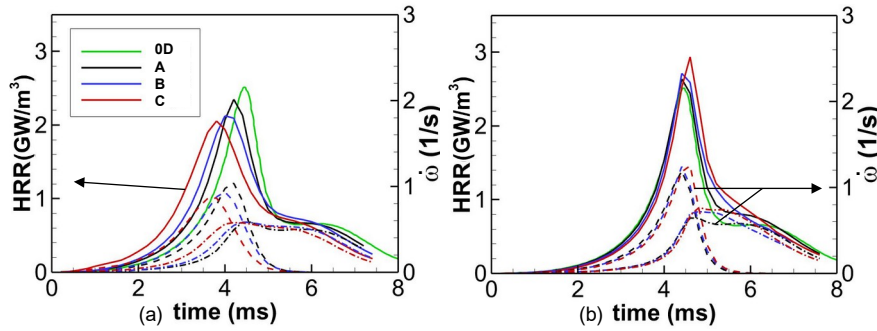


Fig. 3 Temporal evolution of mean HRR (solid lines) and fuel species H_2 (dashed) and CO (dash dot) consumption for variation in stratification for a) thermal stratification b) thermal and compositional stratification

Figure 4 shows the contours of the HRR temporal evolution for cases for various stratification cases. The HRR contour plots are shown at 10%, 50%, and 100% of peak HRR, and one contour is shown where consumption of CO attains a plateau-like nature. The cases with variation in thermal stratification as well as compositional stratification are shown here.

A Da based analysis is a work in progress, so the analysis presented in this paper is limited to the visual identification of modes. The concentric contour with peak HRR at the center can be considered for volumetric igniting mixtures. Multiple flame-like structures also surround the ignition spots. These flame-like structures can be called as deflagration waves. For case A, at 10 % of peak HRR, the HRR contours are uniformly distributed across the domain. Multiple sites with igniting mixtures and deflagration structures can also be seen. With an increase in l_T/l_d (case A to B) and T' (case A to C), the number of ignition sites are observed to be reduced. In contrast, an increase in peak values of available ignition spots can be observed. The higher HRR enhancement is observed with an increase in T' compared to enhancement due to l_T/l_d .

With an increase in l_T/l_d , the scalar gradient within the mixture distribution reduces. The reduced scalar gradient will increase the chances of survival of newly formed ignition spots. This enhanced ignition spot might have resulted in larger ignition spots for case B, whereas for case C, the presence of higher temperature spots increases the reactivity of the mixture, resulting in earlier development of ignition spots.

With time increments, the HRR contours evolved with trends similar to trends observed at 10% of peak HRR. The HRR profiles observed for case B are observed to be uniform and diffuse at 50% and 100% of peak HRR. Compared to case A, with an increase in l_T/l_d and T' , the multiple ignition spots with higher peak HRR values are observed. Thinner deflagration waves with higher peak HRR are observed for cases B and C. The HRR contours at the bottom row indicate the HRR distribution at time instant when CO consumption rate was observed to be steady. This contour indicates that for thermally stratified cases (case A-C) the profiles show higher HRR at locations where the reduced HRR was observed at peak HRR contours. This behavior might have been observed because concentrated reaction zones helped the simultaneous oxidation of CO and H₂.

The HRR contours show uniform distribution for compositionally stratified cases compared to thermally stratified cases. Similar to case C, case C-NC also shows multiple ignition fronts. At peak HRR, a large domain area under explosion can be observed. An increase in consumption area can be observed with an increase in ϕ'/ϕ . The contours at an instant when the CO consumption rate was steady show that max HRR is observed at the location where max HRR was observed at peak HRR contour. This behavior might have happened due to the heat released from H₂ consumption, which might have provided energy for CO oxidation. The sudden ignition of H₂ might not have given sufficient time for CO oxidation, resulting in H₂ oxidation followed by CO oxidation.

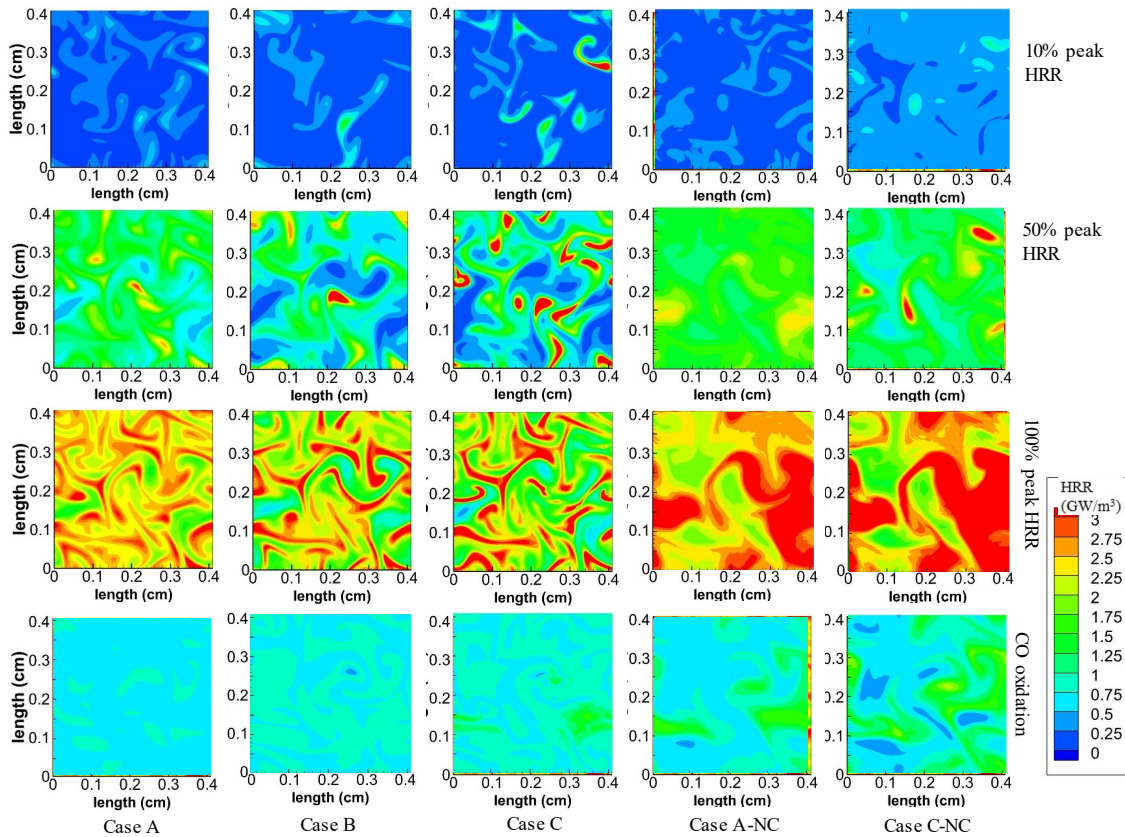


Fig. 4 HRR (GW/m³) contour plot at time instant of 10% (top row), 50% (second row), 100% (third row) of peak HRR for various cases

4. Conclusions

A 2D DNS was performed to analyze the effects of stratification on syngas combustion under HCCI relevant conditions by simulating different levels of stratification. The stratification was mimicked using mixture fields with varying integral scales and fluctuations in temperature and composition. From this work, the following conclusions can be made:

- 1) Autoignition and Species Accumulation:

- 0D simulations revealed that during syngas autoignition, HO₂ species were observed to accumulate sustainably throughout the autoignition.
 - The Damköhler number based on HO₂ can be used to identify two combustion modes: propagating deflagration waves and spontaneous autoignition.
 - The consumption of the fuel species H₂ happened earlier, followed by the consumption of CO.
- 2) Effects of Thermal Stratification:
- An increase in the ratio of integral length scales of temperature to domain size (l_T/l_d) or temperature fluctuations (T') in a thermally stratified mixture led to a shorter and earlier peak in the heat release rate (HRR) with a shallower HRR distribution.
 - With increase in l_T/l_d or T' , H₂ consumption rate followed a similar pattern to HRR, followed by a nearly uniform consumption rate for CO.
- Conversely, in compositionally stratified cases, an increase in the ratio of integral length scales of composition to domain size (l_ϕ/l_d) or composition fluctuations (ϕ'/ϕ) showed a delayed and sharper rise in the HRR profile.
- 3) Ignition Spots and Deflagration Waves:
- Increasing l_T/l_d or T' in a thermally stratified mixture resulted in multiple ignition spots and thinner deflagration waves with higher peak HRR.
- 4) In cases with compositional stratification, combustion characteristics were closer to homogeneous autoignition.

References

- [1] J. Behzadi, M. Bolla, M. Talei, E. R. Hawkes, and S. Kook, "DNS of hydrogen auto-ignition under HCCI-like conditions with wall heat transfer ; parametric study," *Proceedings of the Australian Combustion Symposium*, pp. 1–5, 2015.
- [2] R. N. Roy, M. Muto, and R. Kurose, "Direct numerical simulation of ignition of syngas (H₂/CO) mixtures with temperature and composition stratifications relevant to HCCI conditions," *International Journal of Hydrogen Energy*, vol. 42, no. 41, pp. 26152–26161, 2017.
- [3] M. Talei and E. R. Hawkes, "Ignition in compositionally and thermally stratified n-heptane/air mixtures: A direct numerical simulation study," *Proceedings of the Combustion Institute*, vol. 35, no. 3, pp. 3027–3035, 2015.
- [4] S. Sreedhara and K. N. Lakshmisha, "Autoignition in a non-premixed medium: DNS studies on the effects of three-dimensional turbulence," *Proceedings of the Combustion Institute*, vol. 29, no. 2, pp. 2051–2059, 2002.
- [5] X. J. Gu, D. R. Emerson, and D. Bradley, "Modes of reaction front propagation from hot spots," *Combustion and Flame*, vol. 133, no. 1–2, pp. 63–74, 2003.
- [6] M. M. Ameen and J. Abraham, "Are '2D DNS' results of turbulent fuel/air mixing layers useful for assessing subgrid-scale models?," *Numerical Heat Transfer; Part A: Applications*, vol. 69, no. 1, pp. 1–13, 2016.
- [7] P. Pal, M. Valorani, P.G. Arias "Computational characterization of ignition regimes in a syngas/air mixture with temperature fluctuations," *Proceedings of the Combustion Institute*, vol. 36, no. 3, pp. 3705–3716, 2017.
- [8] S. Karimkashi, H. Kahila, O. Kaario, M. Larmi, and V. Vuorinen, "A numerical study on combustion mode characterization for locally stratified dual-fuel mixtures," *Combustion and Flame*, vol. 214, pp. 121–135, 2020.
- [9] N. Babkovskaia, N. E. L. Haugen, and A. Brandenburg, "A high-order public domain code for direct numerical simulations of turbulent combustion," *Journal of Computational Physics*, vol. 230, no. 1, pp. 1–12, 2011.
- [10] E. R. Hawkes, R. Sankaran, P. P. Pébay, and J. H. Chen, "Direct numerical simulation of ignition front propagation in a constant volume with temperature inhomogeneities: II. Parametric study," *Combustion and Flame*, vol. 145, no. 1–2, pp. 145–159, 2006.
- [11] G. Bansal and H. G. Im, "Autoignition and front propagation in low temperature combustion engine environments," *Combustion and Flame*, vol. 158, no. 11, pp. 2105–2112, 2011.
- [12] J. O. Hinze, *Turbulence*. McGraw-Hill Book Co., New York, 1975.
- [13] C. Olm, I. G. Zsély, T. Varga, H. J. Curran, and T. Turányi, "Comparison of the performance of several recent syngas combustion mechanisms," *Combustion and Flame*, vol. 162, no. 5, pp. 1793–1812, 2015.
- [14] J. Li, Z. Zhao, A. Kazakov, and F. L. Dryer, "An updated comprehensive kinetic model of hydrogen combustion," *International Journal of Chemical Kinetics*, vol. 36, no. 10, pp. 566–575, 2004.

- [15] R. Sankaran and H. G. Im, "Characteristics of auto-ignition in a stratified iso-octane mixture with exhaust gases under homogeneous charge compression ignition conditions," *Combustion Theory and Modelling*, vol. 9, no. 3, pp. 417–432, 2005.
- [16] R. J. Kee, F.M. Rupley, J.A. Miller, *CHEMKIN Collection, Release 3.6*, no. September. San Diego, CA, 2000.
- [17] C. K. Westbrook, "Chemical kinetics of hydrocarbon ignition in practical combustion systems," *Proceedings of the Combustion Institute*, vol. 28, no. 2, pp. 1563–1577, 2000.